DOI: 10.1002/ejic.201100190

Morphology-Tailored Synthesis of PbSe Nanocrystals and Thin Films from Bis[*N*,*N*-diisobutyl-*N*′-(4-nitrobenzoyl)selenoureato]lead(II)

Javeed Akhtar,[a,b] Mohammad A. Malik,[a] Stuart K. Stubbs,[c] Paul O'Brien,*[a] Madeleine Helliwell,[a] and David J. Binks[c]

Keywords: Lead / Selenium / Nanoparticles / Thin films / Chemical vapor deposition

The ligand *N*,*N*-diisobutyl-*N*′-(4-nitrobenzoyl)selenourea (4-NO_2-$C_6H_4CONHCSeNiBu_2$) (**1**) and its complex {bis[*N*,*N*-diisobutyl-*N*′-(4-nitrobenzoyl)selenoureato]lead(II)} [(4-NO_2-$C_6H_4CONHCSeNiBu_2$)Pb^{II}] (**2**) have been synthesized, and their structures determined by single-crystal X-ray methods. Compound **2** was employed as a single-source precursor (SSP) for the deposition of PbSe thin films by aerosol-assisted chemical vapor deposition (AACVD) in the temperature range 250–500 °C on glass substrates. The films obtained at low temperature consist of globular-shaped crystallites, whereas at higher temperature (ca. 500 °C) wirelike morphologies are dominant. PbSe nanocrystals were also prepared from compound **2** by solution thermolysis at 200–250 °C. Photoluminescence (PL) life time measurements based on the time-correlated single-photon-counting (TCSPC) technique showed significantly faster PL decay in as-prepared PbSe nanocrystals relative to previous reports. The purity and elemental composition of the as-deposited PbSe thin films and nanocrystals were determined by energy-dispersive X-ray analysis (EDX).

Introduction

Lead selenide is a IV–VI semiconductor with a small direct band gap (0.27 eV) and large bulk exciton Bohr radius (46 nm).[1] Strong confinement of the electron–hole pair results in a large optical nonlinearity.[2] Lead selenide particles or thin films with critical dimensions best measured in nanometres have potential for application in optical switches,[2–4] communication devices,[5–9] photovoltaic cells,[10–22] biological imaging[23–28] and photodetectors.[29–36] Murray et al first synthesized monodispersed PbSe quantum dots,[37] but a number of other strategies have now been developed.[38–56] Interestingly, all these methods involve the use of separate metal and chalcogenide sources.[38–58]

We have reported the use of [bis(diselenoimidodialkylphosphinato)lead(II)] [$Pb\{N(PR_2Se)_2\}_2$], [bis(dialkylselenophosphinato)lead(II)] [$Pb(R_2PSe_2)_2$] and [bis(diethyldiselenocarbamato)lead(II)] [$Pb(Se_2CNEt_2)_2$] complexes as single-source precursors for the deposition of PbSe thin films by low-pressure LP-CVD and aerosol-assisted (AACVD) experiments.[59–62] However, the deposited films have significant levels of phosphorus contamination with the phosphorus originating from the precursor.[59] Recently, it was shown that cadmium complexes of *N*,*N*-dialkyl-*N*′-acylthiourea or the corresponding *N*,*N*-dialkyl-*N*′-acylselenourea can be used as single-source precursors for the synthesis of CdS or CdSe nanoparticles.[63] Herein, we report the synthesis of a new lead complex, bis[*N*,*N*-diisobutyl-*N*′-(4-nitrobenzoyl)selenoureato]lead(II) [(4-NO_2-$C_6H_4CONHCSeNiBu_2$)Pb^{II}] (**2**), its characterization by single-crystal X-ray crystallography and its use as a single-source precursor for the deposition of phosphorus-free PbSe thin films by AACVD and nanoparticles by solution thermolysis. To the best of our knowledge, this is the first report in which this type of complex is used as a precursor for the deposition of thin films and nanoparticles of PbSe without any phosphorus contamination.

Results and Discussion

Ligand **1** was prepared by a simple method from the reaction of KSeCN, 4-nitrobenzoyl chloride and diisobutylamine at room temperature and its complex **2** from its lead nitrate solution. Both the ligand and lead complex are stable in open atmosphere and can be conveniently stored at room temperature for months. The lead complex is soluble in most organic solvents including toluene or THF. Suitable crystals of **1** and **2** were grown from recrystallization from ethanol and THF/ethanol (1:1), respectively, by slow evaporation of the solvent at room temperature. The crystal structures of compounds **1** and **2** obtained by single-crystal

[a] School of Chemistry and the Materials Science Centre, The University of Manchester,
Oxford Road, Manchester M13 9PL, UK
Fax: +44-161-275-4598
E-mail: paul.obrien@manchester.ac.uk
[b] Present address: Nanoscience and Materials Synthesis Lab, Quaid-i-Azam University,
Islamabad, Pakistan
[c] School of Physics and Astronomy and the Photon Science Institute, The University of Manchester,
Oxford Road, Manchester M13 9PL, UK

X-ray crystallography are shown in Figure 1. The crystal refinement parameters are given in Table 1, while selected bond lengths and bond angles of **2** are given in Table 2.

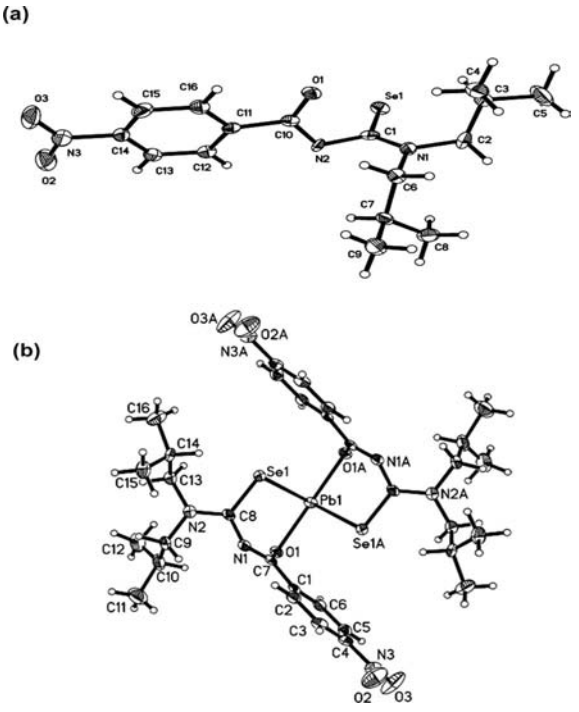

Figure 1. (a) Crystal structure of ligand *N*,*N*-diisobutyl-*N*′-(4-nitrobenzoyl)selenourea. (b) Crystal structure of bis[*N*,*N*-diisobutyl-*N*′-(4-nitrobenzoyl)selenoureato]lead(II).

Crystal Structure of *N*,*N*-Diisobutyl-*N*′-(4-nitrobenzoyl)-selenourea (1)

N,*N*-Diisobutyl-*N*′-(4-nitrobenzoyl)selenourea has a monoclinic space group, *P*2(1)/*c*. The bond length of C=Se (1.824 Å) in this compound is significantly larger than that in the sulfur analogue (1.67 Å).[64–67] This enlargement of the C=Se bond length is due to the bigger size of the Se atom than that of the S atom. There is intermolecular hydrogen bonding between the carbonyl oxygen atom and the hydrogen atom of the selenoamide of the neighbouring molecule [symmetry operators #1: *x*, –*y* + 3/2, *z* + 1/20, N(2)–H(2)···O(1)#1 2.792 Å]. This feature is unusual relative to previous reports,[64–67] where the hydrogen bond is present between the selenium atom of one molecule and the hydrogen atom of the selenoamide of the adjacent molecule, known as resonance-assisted hydrogen bonding (RAHB) or bond cooperativity. The structure of **1** is shown in Figure 1a.

Crystal Structures of Bis[*N*,*N*-diisobutyl-*N*′-(4-nitrobenzoyl)-selenoureato]lead(II) (2)

The structure of the complex **2** shows that each lead atom is surrounded by two selenium and two oxygen atoms, from each chelating *N*,*N*-diisobutyl-*N*′-(4-nitrobenzoyl)selenourea ligand as shown in Figure 1b. The lead atom has a *cis* distorted square-planar geometry. Two of the Pb–Se bonds are significantly longer than the two Pb–O bonds, i.e. Pb(1)–Se(1)#1 2.8577, Pb(1)–Se(1) 2.8578 Å; Pb(1)–O(1)#1 2.428, Pb(1)–O(1) 2.428 Å. This shows that oxygen atoms coordinate more strongly with Pb. The C–N bonds are all

Table 1. Crystal refinement parameters for compounds **1** and **2**.

Empirical formula	$C_{16}H_{23}N_3O_3Se$	$C_{32}H_{44}N_6O_6Se_2Pb$
Formula weight [g mol^{-1}]	384.33	973.84
Temperature [K]	100(2)	100(2)
Wavelength [Å]	0.71073	0.71073
Crystal system, space group	monoclinic, $P2_1/c$	orthorhombic, *Iba*2
a [Å]	7.5909(15)	17.853(3)
b [Å]	24.000(5)	19.592(3)
c [Å]	9.916(2)	10.5264(16)
α [°]	90	90
β [°]	98.320(4)	90
γ [°]	90	90
V [Å^3]	1787.4(6)	3681.9(10)
Z, calculated density [Mg/m^3]	4, 1.428	4, 1.757
Absorption coefficient [mm^{-1}]	2.118	6.608
F(000)	792	1904
Crystal size [mm]	0.25 × 0.20 × 0.04	0.20 × 0.06 × 0.04
θ range for data collection [°]	1.70–28.29	2.08–26.42
Limiting indices	$8 \le h \le 10$, $-29 \le k \le 31$, $-12 \le l \le 9$	$-22 \le h \le 18$, $-24 \le k \le 21$, $-11 \le l \le 13$
Reflections collected/unique	11238/4162 [*R*(int) = 0.1010]	10418/3525 [*R*(int) = 0.0572]
Completeness to *θ* [%]	*θ* = 26.42, 99.8	*θ* = 25.00, 99.4
Max. and min. transmission	0.9201 and 0.6195	1.000 and 0.745
Refinement method	full-matrix least-squares on F^2	full-matrix least-squares on F^2
Data/restraints/parameters	4162/0/212	3525/448/410
Goodness-of-fit on F^2	0.725	1.010
Final *R* indices [$I > 2\sigma(I)$]	*R*1 = 0.0474, *wR*2 = 0.0764	*R*1 = 0.0375, *wR*2 = 0.0613
R indices (all data)	*R*1 = 0.1020, *wR*2 = 0.0876	*R*1 = 0.0621, *wR*2 = 0.0671
Largest diff. peak and hole [e A^{-3}]	0.503 and –0.432	1.043 and –0.434

Table 2. Selected bond lengths [Å] and bond angles [°] for compound **2**.

	Bond length [Å]		Bond angle [°]
Pb(1)–O(1)#1	2.428(6)	O(1)#1–Pb(1)–O(1)	150.0(4)
Pb(1)–O(1)	2.428(6)	O(1)#1–Pb(1)–Se(1)#1	78.95(6)
Pb(1)–Se(1)#1	2.857(1)	O(1)–Pb(1)–Se(1)#1	80.42(8)
Pb(1)–Se(1)	2.857(1)	O(1)–Pb(1)–Se(1)#1	80.42(8)
Pb(1)–O(1)#1	2.428(6)	O(1)#1–Pb(1)–Se(1)	80.42(8)
Pb(1)–O(1)	2.428(6)	O(1)–Pb(1)–Se(1)	78.95(6)
Pb(1)–Se(1)#1	2.857(1)	Se(1)#1–Pb(1)–Se(1)	92.22(5)
C(8)–Se(1)–Pb(1)	101.2(3)°	Se(1)#1–Pb(1)–Se(1)	92.22(5)

shorter than the average C–N bond with a length of 1.472(5) Å as shown in Table 2.[64] The alkyl-substituted selenourea C–N bond [C9–N2 1.475(8) Å] is significantly longer than the amide bond [C7–N1 1.327(4) Å] and the acyl-substituted selenourea C–N bond [C8–N1 1.335(9) Å]. This trend is opposite to that seen for the seleno-palladium and sulfur analogues.[65–67]

Thermogravemetric Analysis

Mass losses in multiple steps between 152–370 °C were observed in the thermogravimetric analysis (TGA) (N_2 atmosphere at 10 °C min^{-1}) of compound **2** (Figure 4a). The mass of the residue obtained from complex **2** is 38.5%, which is close to the theoretically predicted value of 37.30%.

PbSe Thin Films

Deposition was carried out between 200 and 500 °C with an argon flow rate of 160 sccm for 1 h at atmospheric pressure. The reactor was purged with argon for 10 min at the required deposition temperature before deposition was carried out in order to avoid any in situ oxidation. The deposited grey/black films of PbSe weakly adhere to the substrate. The films deposited were analyzed by using XRD, which conclusively shows the formation of the normal cubic form of PbSe (ICDD: 06–3540) at all deposition temperatures (Figure 2). The films were highly textured along the (200) plane. The films deposited show different morphologies at different growth temperatures. The PbSe thin films obtained at 300 °C consist of globular crystallites with a size of ca. 3 μm (Figure 3a). As the growth temperature was increased to 400 °C, two morphologies were observed on the same substrate, which could be a consequence of the temperature gradient in the heating furnace. At the edges of the substrate, the film consists of cubic particles (Figure 3b), which have wirelike structures growing out of their exposed faces. The insert in Figure 3b shows a HR-SEM image of such particles. In the middle of the same film, a network of wirelike structures can be observed (Figure 3c). At 450 °C, the films have irregular, flakelike structures with a micron-size diameter, randomly distributed over the surface (Figure 4d). The films obtained at 500 °C comprise disordered network of wires (Figure 3e, f). Quantitative EDAX analysis confirms that all deposited films have a slight excess of selenium (1–3%) relative to lead.

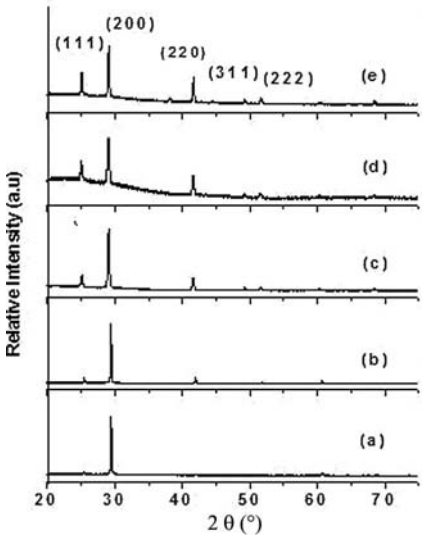

Figure 2. XRD pattern of the as-deposited PbSe thin films from precursor **2** at (a) 300, (b) 350, (c) 400, (d) 450 and (e) 500 °C.

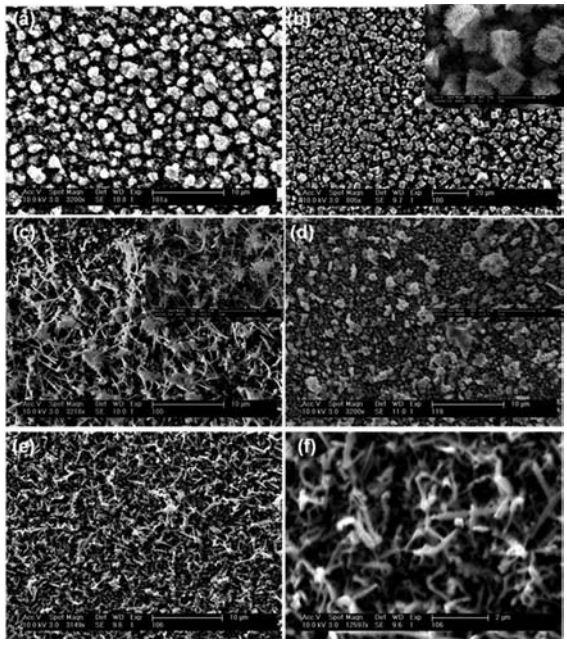

Figure 3. SEM images of PbSe thin films deposited from compound 2 at (a) 300, (b,c) 400, (d) 450, (e,f) 500 °C.

PbSe Nanoparticles

The pXRD pattern of the as-prepared PbSe nanoparticles at 200 °C (Figure 4b) shows a cubic (fcc) lead selenide structure (ICCD: 06-3540). The characteristic cubic pattern with (111), (200), (220), (311), (400) and (420) diffraction peaks is seen. The broadening of the peaks is consistent with the small size of the PbSe nanoparticles. At 200 °C, nearly spherical PbSe nanoparticles form. The size of the nanoparticles calculated by Scherrer's equation is 11.5 nm, which is close to the average diameter obtained from the TEM image, 11.8 nm ± 1.9 (Figure 5a–c). At 250 °C, the predominate morphology of PbSe is cubic (18.4 nm ± 3.1 nm), as shown in Figure 5d–f. The EDAX profile of the as-prepared PbSe nanoparticles shows the presence of only Pb and Se in an almost 1:1 ratio.

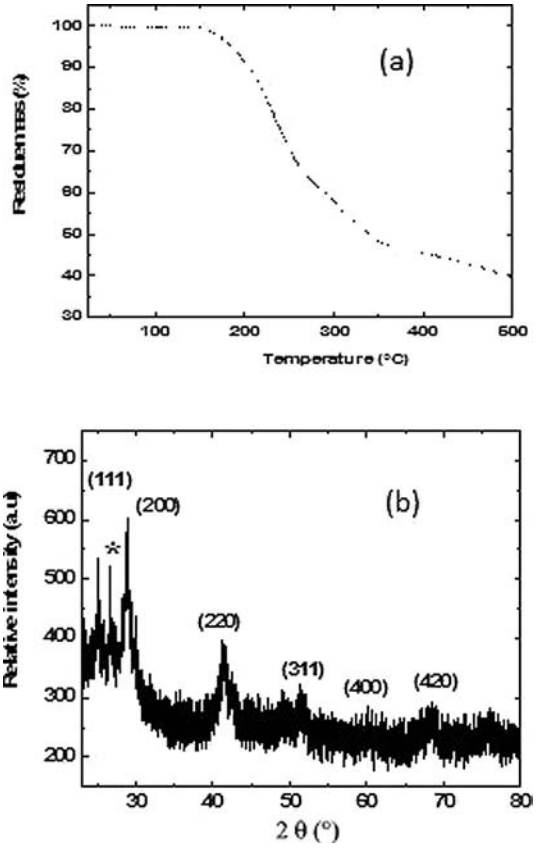

Figure 4. (a) Thermogravimetric analysis (TGA) for **2** at a heating rate of 10 °C/min under a nitrogen flow rate of 100 mL/min. (b) Typical pXRD of PbSe nanoparticles prepared by thermolysis of **2** at 200 °C.

The electronic spectrum of the PbSe nanoparticles shows a band edge at 950 nm, 1.3 eV (Figure 6a). There is a considerable blueshift in the absorption spectrum of the as-synthesized PbSe relative to that of the bulk (4.6 μm, 0.27 eV). A PL life time experiment based on the time-correlated single-photon-counting (TCSPC) technique was carried out on the as-prepared PbSe nanoparticles synthesized at 200 °C. The PL transient obtained is well described by a triexponential decay; both the experimental data and the fitted triexponential function are shown in Figure 6b. The decay constants associated with the fit are 10 ± 1, 3.0 ± 0.2 and 0.71 ± 0.01 ns; the relative amplitudes of the constants are 8, 35 and 57%, respectively. The PL decay observed here is significantly faster than that reported previously for PbSe nanoparticles;[68] in that case, a largely monoexponential decay with a 880-ns time constant was observed and attributed to electron–hole pair recombination. The multiexponential form and the much-more-rapid decay observed in the current study suggest that processes other than electron–hole pair recombination are significant.

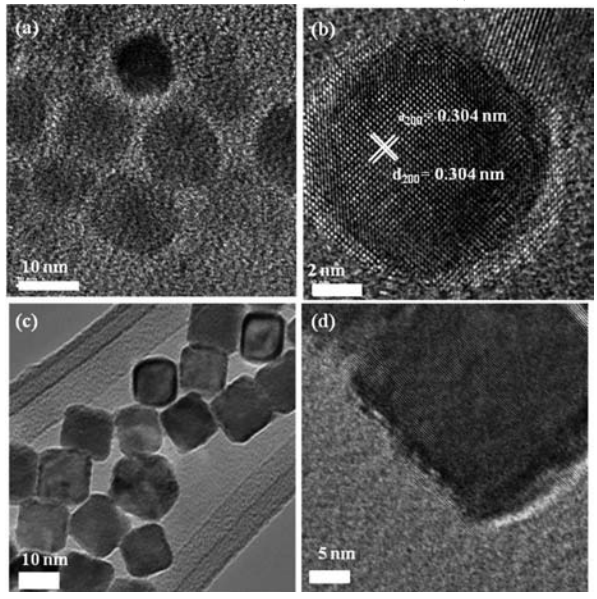

Figure 5. (a–c) spherical PbSe nanoparticles prepared from precursor **2** at 200 °C, (d–f) cubic PbSe nanoparticles prepared at 250 °C (all in TOP/oleicacid/octadecene).

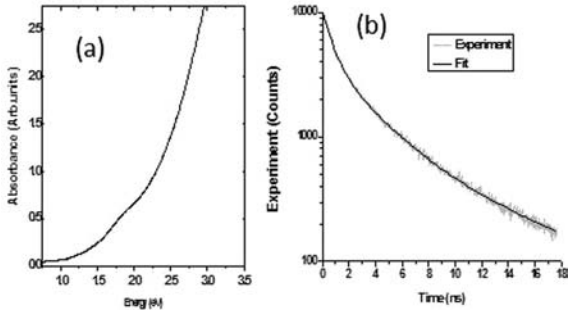

Figure 6. (a) UV/Vis absorption spectrum of the PbSe nanoparticles prepared from precursor **2**. (b) Fluorescence lifetime decay curves of PbSe nanoparticles prepared from precursor **2**.

Conclusions

The ligand *N*,*N*-diisobutyl-*N*′-(4-nitrobenzoyl)selenourea and its lead complex have been characterized by single-crystal X-ray crystallography. The lead complex **2** deposited thin films of various morphologies at temperatures between 300 and 500 °C. Nanoparticles grown by the thermolysis of the complex in TOP (trioctylphosphane), octadecene or

oleic acid at 200 °C gave spherical particles, whilst the growth at 250 °C resulted in cubes. The pXRD of both the thin films and nanoparticles showed cubic PbSe. The nanocrystals can easily be dispersed in organic solvents such as toluene or hexane.

Experimental Section

General: All synthetic preparations were performed under an inert atmosphere of dry nitrogen by using standard Schlenk line techniques. All reagents were purchased from Sigma–Aldrich and used as received. Solvents were distilled and dried prior to use as necessary. ^{1}H NMR spectra were obtained by using a Bruker AC300 FT-NMR spectrometer. Mass spectra were recorded on a Kratos concept 1S instrument. Infrared spectra were obtained on a Specac single-reflectance ATR instrument (4000–400 cm^{-1}). Elemental analysis was performed by the University of Manchester microanalytical facility. TGA was carried out by using a Seiko SSC/S200 thermal analyzer with a heating rate of 10 °C min^{-1} under nitrogen with flow rate of 100 mL per minute.

Thin films of lead chalcogenide material were deposited by using a home-built AACVD reactor.[69] X-ray powder diffraction patterns were obtained by using a Bruker D8 AXE diffractometer (with Cu-K_α radiation). The samples were scanned between 20 and 80 ° (step size of 0.05 °, with a count rate of 9 s). Thin films were carbon coated by using an Edwards E-306A coating system before carrying out SEM and EDX analysis. SEM was performed with a Philips XL 30FEG and EDX analysis were carried out with a DX4 instrument. TEM samples were prepared by evaporating a dilute toluene solution of the nanoparticles onto carbon-coated copper grids (S160–3, Agar Scientific), and a Tchnai transmission electron microscope (TEM) was used to obtain TEM images of the nanoparticles.

A time-correlated single-photon-counting instrument (MiniTau, Edinburgh Instruments) was used to determine the PL lifetimes. A diode laser emitting pulses with a 90-ps duration at 405 nm (EPL-405, Edinburgh Instruments) was used to excite the sample; scattered excitation light was suppressed by using a long-pass filter that cuts off wavelengths shorter than 600 nm. The PL decay transient was measured with a commercial time-correlated single-photon-counting instrument (MiniTau, Edinburgh Instruments). PL was detected by using a photomultiplier tube (H4722, Hammatsu), and the instrument response function of the system had a full-width-half-maximum of better than 300 ps.

Synthesis: The preparation of ligand **1** and its lead complex **2** were carried out by modification of the methods reported in literature[70,71] and are detailed in Scheme 1. Briefly, an acetone solution of 4-nitrobenzoyl chloride (4.5 g, 24 mmol in 30 mL) was added into an acetone solution of KSeCN (3.5 g, 24 mmol, in 30 mL) at room temperature in a 250-mL two-neck flask under nitrogen. The contents of the flask changed colour from white to greenish–yellow. The mixture was stirred for 5 min at room temperature to ensure completion of reaction. Addition of diisobutylamine (4.2 mL, 24 mmol in 10 mL acetone) solution into the mixture resulted in a change of colour from dirty green to orange red. After another 5 min of stirring at room temperature, anhydrous ether (50 mL) was added, and the flask was left undisturbed for 5 min. The *N*,*N*-diisobutyl-*N*′-(4-nitrobenzoyl)selenourea was extracted into ether and separated in a funnel. Upon evaporation of the ether solution, the red solid residue obtained was re-crystallized from ethanol to give green cubic crystals of *N*,*N*-diisobutyl-*N*′-(4-nitrobenzoyl)-selenourea (**1**). Yield: 29%. Elemental analysis: calcd. C 50.0, H 6.0, N 10.9%; found C 48.7, H 5.3, N 10.3%. IR: 2986 υ(C–H), 1732 υ(C=O), 1079 υ(C=Se), 1223 υ(C–N) cm^{-1}. ^{1}H NMR ($CDCl_3$, 400 MHz): δ = 0.89 (m, 6 H), 1.10 (m, 6 H), 2.1 (t, 2 H), 2.3 (t, 2 H), 3.4 (d, 2 H), 8.1(d, Ar, 2 H), 8.2 (s, N–H), 8.38 (d, Ar, 2 H) ppm. MS (ES, negative scan): *m*/*z* (%) = 383 (100).

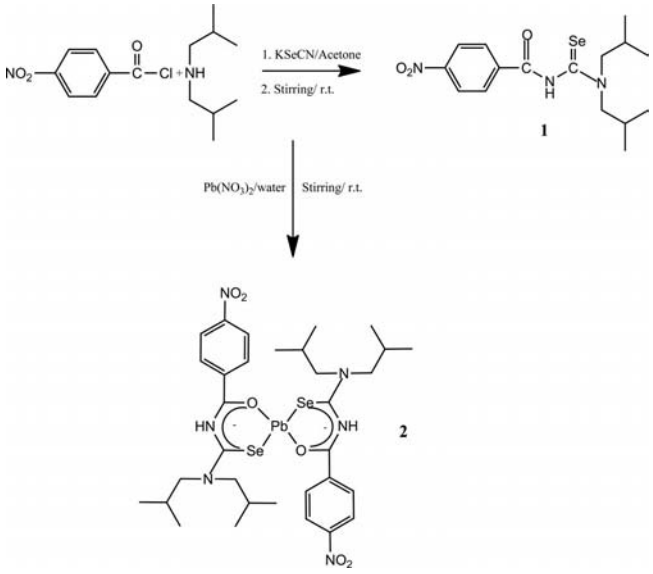

Scheme 1. Synthetic scheme for bis[*N*,*N*-diisobutyl-*N*′-(4-nitrobenzoyl)selenoureato]lead(II).

An ethanol solution of ligand **1** (1 g, 2.6 mmol in 40 mL) with lead nitrate (0.43 g, 1.3 mmol) in the presence of sodium acetate (0.43 g, 5.2 mmol) in water (10 mL) at room temperature gave a yellow precipitate of bis[*N*,*N*-diisobutyl-*N*′-(4-nitrobenzoyl)selenoureato]-lead(II) (**2**). Yield: 54%. Elemental analysis: calcd. C 39.4, H 4.5, N 8.6, Pb 21.3%; found C 39.7, H 4.6, N 8.74, Pb 19.9%. IR: 3064 υ(C–H), 1645 υ(C=O), 1056 υ(C=Se), 1419 υ(C–N) cm^{-1}. ^{1}H NMR ($CDCl_3$, 400 MHz): δ = 0.74 (d, 12 H), 0.87 (d, 12 H), 1.6 (t, 2 H), 2.1 (t, 2 H), 3.5 (d, 4 H), 3.78(d, 4 H), 8.28(m, Ar, 8 H) ppm. MS (ES^- scan): *m*/*z* (%) = 384 (100).

X-ray Crystallography: Single-crystal X-ray crystallography of compounds **1** and **2** was carried out on a Bruker APEX diffractometer by using graphite monochromated Mo-K_α radiation (λ = 0.71073 Å). The structure was solved by direct methods and refined by full-matrix least-squares on F^2.[72] All non-H atoms were refined anisotropically. H atoms were placed in calculated positions by assigned isotropic thermal parameters and allowed to ride on their parent carbon atoms. All calculations were carried out by using the SHELXTL package.[73] CCDC-685384 (for **1**) and -733567 (for **2**) contain the supplementary crystallographic data for this paper. These data can be obtained free of charge from The Cambridge Crystallographic Data Centre via www.ccdc.cam.ac.uk/data_request/cif.

Deposition of Thin Films by AACVD: In a typical deposition experiment, the precursor (0.20 g, 0.8 mmol) was dissolved in toluene (12 mL) in a two-necked 100-mL round-bottomed flask with a gas inlet that allows the carrier gas (argon) to pass into the solution and to aid transport of the aerosol. This flask was connected to the reactor tube by a piece of reinforced tubing. The argon flow rate was controlled by a Platon flow gauge. Six glass substrates (approx. 1 × 3 cm) were placed inside the reactor tube and placed

in a Carbolite furnace. The precursor solution in a round-bottomed flask was kept in a water bath above the piezoelectric modulator of a PIFCO ultrasonic humidifier (Model No. 1077). The aerosol droplets of the precursor thus generated were transferred into the hot-wall zone of the reactor by carrier gas, where the precursor decomposes to deposit a thin film of the required material.

PbSe Nanoparticles by the Colloidal Method: TOP (12.7 g) and oleic acid (1 mL) along with octadecene (4 mL) were placed in three-neck flask and heated to 100 °C under vacuum for 30 min. The flask was then flushed with nitrogen and again exposed to a vacuum for 5 min. This procedure was repeated three times and heating was continued until 200 °C, after which the temperature was maintained. Bis[*N*,*N*-diisobutyl-*N*′-(4-nitrobenzoylselenoureato)lead(II)] (0.70 g) was then dissolved in TOP (3 mL), and octadecene (1 mL) was rapidly injected. The colour of the mixture changed instantaneously from yellow to black–brown. The hot reaction flask was removed from the heating mantle within 60 s and was allowed to cool at room temperature. The addition of acetone (20 mL) into the flask gave a blackish precipitate, which was separated by centrifugation. The obtained material appeared as brown jelly and was suspended in toluene (5 mL) and re-precipitated by adding an excess of acetone to wash away any impurities and excess coating. The purified nanoparticles stayed suspended in toluene without any coagulation for several weeks. The same reaction was repeated at higher temperature of 250 °C.

Acknowledgments

Javeed Akhtar thanks the Higher Education Commission (HEC) of Pakistan for financial assistance, and we all thank the EPSRC for funding. P. O. B. wrote this manuscript while a visiting fellow at the IAS University of Durham. He would like to thank the University for the Fellowship and Collingwood College and its fellows for being gracious hosts.

[1] B. R. Hyun, H. Chen, D. A. Rey, F. W. Wise, C. A. Batt, *J. Phys. Chem. B* **2007**, *111*, 5726.
[2] F. W. Wise, *Acc. Chem. Res.* **2000**, *33*, 773.
[3] R. P. Watekar, A. Lin, S. Ju, W. T. Han, *Opt. Fiber Commun. Conf. (OFC)*, **2008**, 1.
[4] M. Brumer, M. Sirota, A. Kigel, A. Sashchiuk, E. Galun, Z. Burshtein, E. Lifshitz, *Appl. Opt.* **2006**, *45*, 7488.
[5] P. T. Guerreiro, S. Ten, N. F. Borrelli, J. Butty, G. E. Jabbour, N. Peyghambarian, *Appl. Phys. Lett.* **1997**.*71*, 1595.
[6] J. Ethan, D. Klem, L. Levina, E. H. Sargent, *Appl. Phys. Lett.* **2005**, *87*, 053101.
[7] J. S. Steckel, S. Coe-Sullivan, V. Bulovic, M. G. Bawendi, *Adv. Mater.* **2003**, *15*, 1862.
[8] C. E. Finlayson, A. Amezcua, P. J. A. Sazio, P. S. Walker, *J. Mod. Opt.* **2005**, *52*, 955.
[9] D. V. Talapin, C. B. Murray, *Science* **2005**, *310*, 86.
[10] J. M. Luther, M. Law, Q. Song, C. L. Perkins, M. C. Beard, A. J. Nozik, *ACS Nano* **2008**, *2*, 271.
[11] J. P. Clifford, K. W. Johnston, L. Levina, E. H. Sargent, *Appl. Phys. Lett.* **2007**, *91*, 2531171.
[12] V. Sholin, A. J. Breeze, I. E. Anderson, Y. Sahoo, D. Reddy, S. A. Carter, *Sol. Energy Mater. Sol. Cells* **2008**, *92*, 1706.
[13] A. Bhardwaj, V. R. Balakrishnan, P. Srivastava1, H. K. Sehgal1, *Semicond. Sci. Technol.* **2008**, *23*, 095020.
[14] S. J. Kim, W. J. Kim, Y. Sahoo, A. N. Cartwright, P. N. Prasad, *Appl. Phys. Lett.* **2008**, *92*, 031107.
[15] D. Yun, W. Feng, H. Wu, K. Yoshino, *Sol. Energy Mater. Sol. Cells* **2009**, *93*, 1208.
[16] B. Vercelli, G. Zotti, A. Berlin and M. Natali *Chem. Mater.* **2010**, ASAP Article, DOI: 10.1021/cm903824e.
[17] K. S. Leschkies, T. J. Beatty, M. S. Kang, D. J. Norris, E. S. Aydil, *ACS Nano* **2009**, *3*, 3638.
[18] M. W. Luther, J. M. Zheng, H. Wu, A. P. Alivistos, *Nano Lett.* **2009**, *9*, 1699.
[19] G. I. Koleilat, L. Levina, H. Shukla, S. H. Myrskog, S. Hinds, A. G. Pattantyus-Abraham, E. H. Sargent, *ACS Nano* **2008**, *2*, 833.
[20] W. Ma, J. M. Luther, H. Zheng, Y. Wu, A. P. Alivisatos, *Nano Lett.* **2009**, *9*, 1699.
[21] M. Law, M. C. Beard, S. Choi, J. M. Luther, M. C. Hanna, A. J. Nozik, *Nano Lett.* **2008**, *8*, 3904.
[22] C. Y. Liu, Z. C. Holman, U. R. Kortshagen, *Nano Lett.* **2009**, *9*,449.
[23] R. D. Schaller, M. A. Petruska, V. I. Klimov, *J. Phys. Chem. B* **2003**, *107*, 13765.
[24] C. M. Evans, L. Guo, J. J. Peterson, S. M. Zacher, T. D. Krauss, *Nano Lett.* **2008**, *8*,2896.
[25] B. R. Hyun, H. Chen, D. A. Rey, F. W. Wise, C. A. Batt, *J. Phys. Chem. B* **2007**, *111*, 5726.
[26] G. Yao, L. H. V. Wang, *Phys. Med. Biol.* **1999**, *44*, 2307.
[27] R. K. K. Wang, *Phys. Med. Biol.* **2002**, *47*, 2281.
[28] Y. T. Lim, S. Kim, A. Nakayama, N. E. Stott, M. G. Bawendi, J. V. Frangioni, *Mol. Imaging* **2003**, *2*, 50.
[29] K. Kellermann, D. Zimin, K. Alchalabi, P. Gasser, H. Zogg, *Physica E* **2004**, *20*, 536.
[30] A. Munoz, J. Melendez, M. C. Torquemada, M. T. Rodrigo, *Thin Solid Films* **1998**, *317*, 425.
[31] V. V. Tetyorkin, A. Y. Sipatov, F. F. Sizov, A. I. Fedorenko, A. A. Fedorov, *Infrared Phys. Technol.* **1996**, *37*, 379.
[32] T. Beyer, M. Tacke, *Appl. Phys. Lett.* **1998**, *73*, 1191.
[33] J. M. Martin, J. L. Hernández, L. Adell, A. Rodriguez, F. López, *Semicond. Sci. Technol.* **1996**, *11*, 1740.
[34] E. H. Sargent, *Adv. Mater.* **2005**, *17*, 515.
[35] J. P. Clifford, G. Konstantatos, K. W. Johnston, S. Hoogland, L. Levina, E. H. Sargent, *Nat. Nanotechnol.* **2009**, *4*, 40.
[36] G. Konstantatos, J. Clifford, L. Levina, E. H. Sargent, *Nature Photon.* **2007**, 1,531.
[37] C. B. Murray, S. W. Shouheng, D. H. Gaschler, T. A. Betley, C. R. Kagan, *IBM J. Res. Dev.* **2001**, *45*, 47.
[38] M. Brumer, A. Kigel, L. Amirav, A. Sashchiuk, O. Solomesch, N. Tessler, E. Lifshitz, *Adv. Funct. Mater.* **2005**, *15*, 1111.
[39] H. Tong, L. X. Yang, L. Li, L. Zhang, J. Y. Zhu, *Angew. Chem.* **2006**, *118*, 7903; *Angew. Chem. Int. Ed.* **2006**, *45*, 7739.
[40] K. L. Hull, J. W. Grebinski, T. H. Kosel, M. Kuno, *Chem. Mater.* **2005**, *17*, 4416.
[41] M. J. Bierman, Y. K. Albert Lau, S. Jin, *Nano Lett.* **2007**, *7*, 2907.
[42] T. Ji, W. B. Jian, J. Fang, *J. Am. Chem. Soc.* **2003**, *125*, 8448.
[43] L. Carbone, S. Kudera, C. Giannini, G. Ciccarella, R. Cingolani, P. D. Cozzoli, L. Manna, *J. Mater. Chem.* **2006**, *16*, 3952.
[44] A. J. Houtepen, R. Koole, D. Vanmaekelbergh, J. Meeldijk, S. G. Hickey, *J. Am. Chem. Soc.* **2006**, *128*, 6792.
[45] W. Lu, P. Gao, W. B. Jian, Z. L. Wang, J. Fang, *J. Am. Chem. Soc.* **2004**, *126*, 14816.
[46] S. Kudera, L. Carbone, M. F. Casula, R. Cingolani, A. Falqui, E. Snoeck, W. J. Parak, L. Manna, *Nano Lett.* **2005**, *5*, 445.
[47] W. Wang, Y. Geng, Y. Qian, M. Ji, X. Liu, *Adv. Mater.* **1998**, *10*, 1479.
[48] W. W. Yu, J. C. Falkner, B. S. Shih, V. L. Colvin, *Chem. Mater.* **2004**, *16*, 3318.
[49] W. Lu, Y. Ding, Z. L. Wang, J. Fang, *J. Phys. Chem. B* **2005**, *109*, 19219.
[50] E. Lifshitz, M. Brumer, A. Kigel, A. Sashchiuk, M. Bashouti, M. Sirota, E. Galun, Z. Burshtein, A. Q. Le Quang, I. Ledoux-Rak, J. Zyss, *J. Phys. Chem. B* **2006**, *110*, 25356.
[51] M. Klokkenburg, A. J. Houtepen, R. Koole, J. W. J. de Folter, B. H. Erné, E. van Faassen, D. Vanmaekelbergh, *Nano Lett.* **2007**, *7*, 2931.
[52] W. Zhu, W. Wang, J. Shi, *J. Phys. Chem. B* **2006**, *110*, 9785.
[53] J. P. Ge, Y. D. Li, *J. Mater. Chem.* **2003**, *13*, 911.

[54] X. Wang, J. Zhuang, Q. Peng, Y. Li, *Langmuir* **2006**, *22*, 7364.
[55] J. Xu, J. P. Ge, Y. D. Li, *J. Phys. Chem. B* **2006**, *110*, 2497.
[56] J. Zhu, H. Peng, C. K. Chan, K. Jarausch, X. F. Zhang, Y. Cui, *Nano Lett.* **2007**, *7*, 1095.
[57] J. B. Mullin, S. C. J. Irvine, D. J. Ashen, *J. Cryst. Growth* **1981**, *55*, 92.
[58] B. Manfred, P. C. Andrew, K. P. Annie, *Polyhedron* **1992**, *11*, 507.
[59] a) M. Afzaal, E. Katie, P. L. Nigel, P. O'Brien, J. Raftery, J. Waters, *J. Mater. Chem.* **2004**, *14*, 1310; b) M. Afzaal, D. Crouch, M. A. Malik, M. Motevalli, P. O'Brien, J.-H. Park, J. D. Woolins, *Eur. J. Inorg. Chem.* **2004**, *1*, 171; c) J. Waters, D. Crouch, J. Raftery, P. O'Brien, *Chem. Mater.* **2004**, *16*, 3289.
[60] T. Trindade, O. C. Monterio, P. O'Brien, M. Motevalli, *Polyhedron* **1999**, *18*, 1171.
[61] F. Dongbo, M. A. Malik, N. Q. Chin, P. O'Brien, J. P. Thomas, *Coord. Chem. Rev.* **2007**, *251*, 1878.
[62] J. S. Ritch, T. Chivers, K. Ahmad, M. Afzaal, P. O'Brien, *Inorg. Chem.* **2010**, *49*, 1198.
[63] J. C. Bruce, N. Revaprasadu, K. R. Koch, *New J. Chem.* **2007**, *31*, 1647.
[64] J. C. Bruce, K. R. Koch, *Acta Crystallogr., Sect. C* **2008**, *64*, m1.
[65] J. Dillen, M. G. Woldu, K. R. Koch, *Acta Crystallogr., Sect. E: Struct. Rep. Online* **2006**, *62*, o5228.
[66] J. Dillen, M. G. Woldu, K. R. Koch, *Acta Crystallogr., Sect. E: Struct. Rep. Online* **2006**, 62, o4819.
[67] W. Bensch, M. Schuster, *Z. Anorg. Allg. Chem.* **1994**, 620,1479.
[68] B. L. Wehrenberg, C. Wang, P. Guyot-Sionnest, *J. Phys. Chem. B* **2002**, *106*, 10634.
[69] G. Horley, M. Lazell, P. O'Brien, *Chem. Vap. Deposition* **1996**, *2*, 242.
[70] I. B. Douglass, *J. Am. Chem. Soc.* **1937**, *59*, 740.
[71] I. B. Douglass, F. B. Dains, *J. Am. Chem. Soc.* **1934**, *56*, 1408.
[72] G. M. Sheldrick, *SHELXL 97* and *SHELXS 97*, University of Gottingen, Germany, **1997**.
[73] *SHELTXTL Version 6.10*, Bruker AXS Inc., Madison, Wisconsin, USA, **2000**.

Received: February 24, 2011
Published Online: May 24, 2011

